Bullet Impact on Steel and Kevlar®/Steel Armor - Computer Modeling and Experimental Data*

Dale S. Preece
Sandia National Laboratories
P.O. Box 5800
Albuquerque, NM 87185-1156

Vanessa S. Berg
Sandia National Laboratories
P.O. Box 5800
Albuquerque, NM 87185-1156

ABSTRACT

Computer hydrocode analyses and ballistic testing have been used to investigate the effectiveness of steel plate armor against lead/copper bullets commonly available in the U.S. and across the world. Hydrocode simulations accurately predict the steel plate thickness that will prevent full penetration as well as the impact crater geometry (depth and diameter) in that thickness of steel armor for a 338 caliber bullet. Using the hydrocode model developed for steel armor, studies were also done for an armor consisting of a combination of Kevlar® and steel. These analyses were used to design the experiments carried out in the ballistics lab at Sandia National Laboratories.

Ballistics lab testing resulted in a very good comparison between the hydrocode computer predictions for bullet impact craters in the steel plate armor and those measured during testing. During the experiments with the combination armor (Kevlar®/steel), the steel became a witness plate for bullet impact craters following penetration of the Kevlar®. Using the bullet impact craters in the steel witness plate it was determined that hydrocode predictions for Kevlar® armor are less accurate than for metals. This discrepancy results from the inability of the hydrocode (Eulerian) material model to accurately represent the behavior of the fibrous Kevlar®.

Thus, this paper will present the hydrocode predictions and ballistics lab data for the interaction between a lead/copper bullet and several armoring schemes: 1) steel, 2) Kevlar®, and 3) a Kevlar®/steel combination.

INTRODUCTION

Most penetration analyses and armor designs in the past have dealt with cartridges that have military-style steel jacketed and armor-piercing bullets. Body armor studies have typically focused on handgun ammunition. The effect of a typical high-powered rifle hunting bullet on steel and Kevlar® armor will be the focus of this study.

The hunting cartridge chosen for this study was the 338 Winchester Magnum which is commonly used in North America for larger big game such as elk, moose and caribou. An A-frame hunting bullet was chosen for study because it was designed for deep penetration of larger game animals. The A-frame design is constructed from copper and lead as illustrated in Figure 1. Cartridges employing this bullet are readily available in North America in many different calibers. The 338 Winchester was chosen because it is one of the more powerful. As such, this cartridge/bullet combination seems to be a likely candidate for study of the effects of readily available hunting ammunition on Kevlar® armor.

In this study mild steel is used as a witness plate for the effects of the 338 bullet, first on the bare steel and then with several different thicknesses of Kevlar® armor. Penetration of the bullet into a bare mild steel plate is a baseline for judging the effectiveness of the armor when compared to penetration into steel following penetration of the Kevlar®. A computer hydrocode was used to predict the penetration of the 338 Winchester Magnum A-frame bullet into bare mild steel. An assessment of the performance of Kevlar® armor was also performed. These calculations were used to design the experiments performed in the ballistics lab at Sandia National Laboratories. There were two phases of the experimental program. Phase 1 was designed to validate the predictive capability of the computer program AUTODYN (Century Dynamics Inc, 2001) to predict the geometry and depth of a bullet impact on bare steel. Pre-test predictions were close but for Post-test simulations the bullet velocity was changed to match that measured in the lab and the material model was adjusted slightly to better match the experimental results. Phase II was designed to validate predictions of the interaction of the bullet with the Kevlar® armor and then with the steel. A philosophy behind choosing the steel and Kevlar® thickness was prevention of total steel penetration. A total penetration is ambiguous because the configuration and energy remaining in the bullet, upon exit, is unknown.

AUTODYN COMPUTER PREDICTIONS

The AUTODYN (Century Dynamics Inc, 2001) computer code was employed in full Eulerian (material passes through the grid) mode to simulate the bullet impacting the steel. Figure 1 illustrates the AUTODYN model of the bullet. The model consists of 32000 grid cells that are filled with materials as illustrated in Figure 1. The bullet has an A-Frame or partitioned (Nosler Inc., 2002) style that is a common hunting bullet designed for deep penetration of large animals

* This work was performed at Sandia National Laboratories. Sandia is a multi-program laboratory operated by Sandia Corporation, a Lockheed MartinCompany, for the United States Department of Energy under Contract No. DE-AC04-94AL85000.

Published in the Proceedings of the ASME Pressure Vessels and Piping Conference – Symposium on Structures Under Extreme Loading, July 25-29, 2004, San Diego, CA.

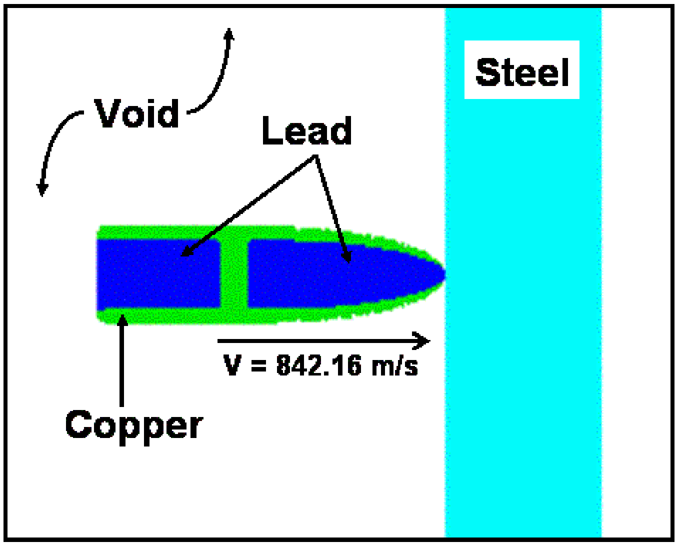

Figure 1. AUTODYN model of a 338 Winchester Magnum A-Frame hunting bullet just prior to impacting the steel. Bullet velocity is 842.16 m/s and the steel thickness is 14.275 mm.

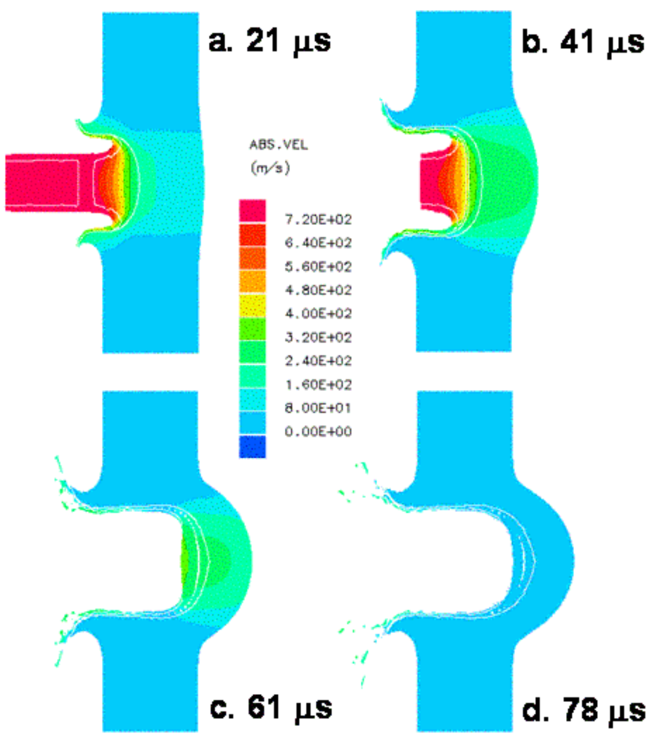

Figure 2. AUTODYN simulation of the bullet from Figure 1 impacting/penetrating the steel plate. Color represents absolute velocity in m/s as indicated by the color bar.

Table 1. Material Properties for Impact Simulations

Property	Value
Lead	
Equation of State	Shock
Reference Density (g/cm^3)	11.35
Gruneisen Coefficient	2.77
Parameter C_1 (m/s)	2.051E03
Parameter S_1	1.46
Strength Model	Von Mises
Shear Modulus (KPa)	5.6E6
Yield Strength (KPa)	5.0E3
Copper	
Equation of State	Shock
Reference Density (g/cm^3)	8.93
Gruneisen Coefficient	1.99
Parameter C_1 (m/s)	3.94E03
Parameter S_1	1.489
Strength Model	Von Mises
Shear Modulus (KPa)	4.5E7
Yield Strength (KPa)	7.0E4
Kevlar®	
Equation of State	Puff
Reference Density (g/cm^3)	1.29
Parameter A_1 (kPa)	8.21E06
Parameter A_2 (kPa)	7.036E07
Parameter A_3 (kPa)	0.0
Gruneisen Coefficient	0.35
Expansion Coefficient	0.25
Sublimation Energy (J/Kg)	8.23E06
Parameter T_1 (kPa)	0.0
Parameter T_2 (kPa)	0.0
Reference Temp (K)	0.0
Specific Heat (C.V.) (J/kgK)	0.0
Strength Model	Von Mises
Shear Modulus	3.0E7
Yield Strength	3.0E5
Tensile Strength	-2.6E5
Steel	
Equation of State	Shock
Strength Model	Johnson-Cook
Reference Density (g/cm^3)	7.896
Gruneisen Coefficient	2.17
Parameter C_1 (m/s)	4.569E03

Table 1 - Steel (Cont.)	
Parameter S_1	1.49
Reference Temperature (K)	300
Shear Modulus (kPa)	8.18E07
Yield Stress (kPa)	5.17106E05
Hardening Constant (kPa)	2.75E05
Hardening Exponent	0.36
Strain Rate Constant	0.022
Thermal Softening Exponent	1.0
Melting Temperature (K)	1.811E03

such as moose and elk. Material properties of the lead, copper and steel employed in this simulation are given in Table 1. During penetration of flesh, the nose of the bullet peels back to the copper partition and then remains intact as penetration continues. The copper partition makes only a small difference when penetrating steel.

Figure 2 shows the simulation of bullet impact/penetration at times 21, 41, 61, and 78 µs. The final penetration that is compared to experimental results is shown in Figure 2d and Figure 3. Dimensions of the predicted impact crater are given in Figure 3. As will be seen in the experimental data given later, the lead and copper did not usually adhere to the inside surface of the impact crater as indicated in the simulation but was often found loose and basically intact within the crater. Therefore the measurements from the experiments were to the steel at the base of the crater and from steel to steel at the mouth of the crater.

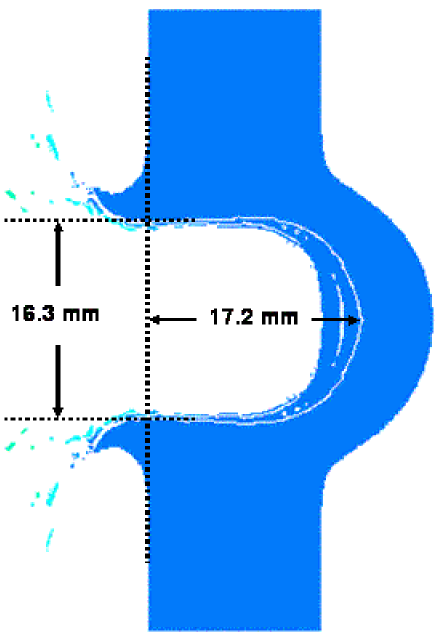

Figure 3. Impact crater dimensions from Figure 2d. Measurements are made to steel surfaces.

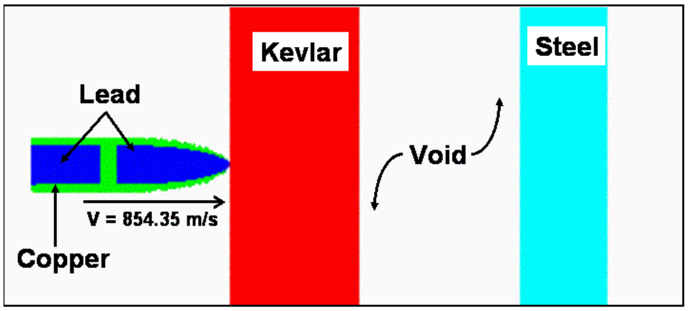

Figure 4. AUTODYN model of a 338 Winchester Magnum A-Frame hunting bullet just prior to impacting the Kevlar® Armor. Bullet velocity is 854.35 m/s (2763 ft/s), Kevlar® thickness is 20 mm (0.787 inches) and the steel thickness is 14.275 mm (0.562 inches).

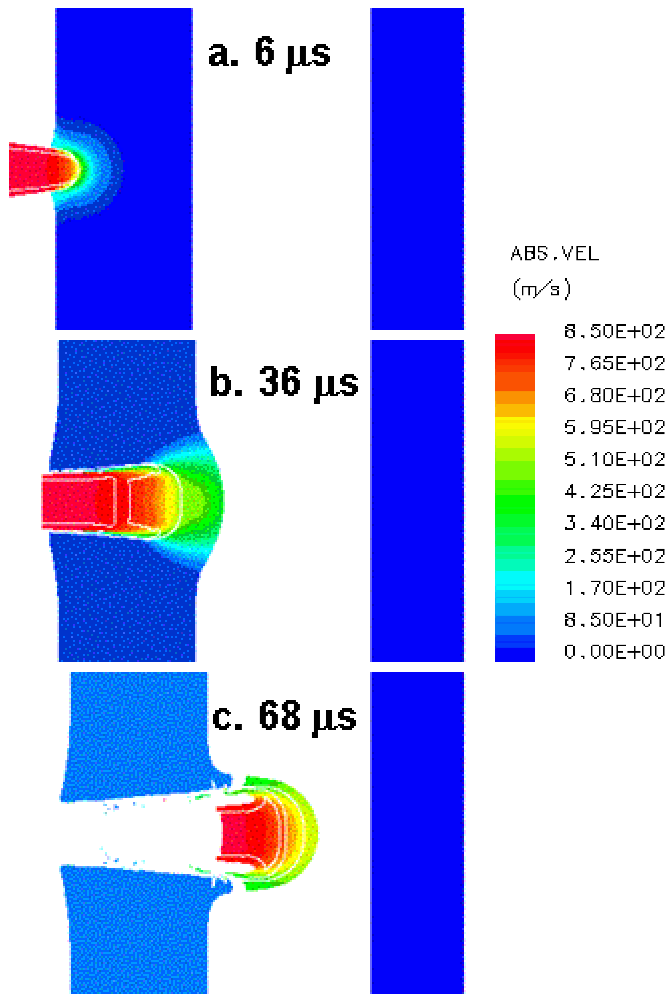

Figure 5. AUTODYN simulation of the bullet from Figure 4 impacting/penetrating the Kevlar® armor. Color represents absolute velocity in m/s as indicated by the color bar. Kevlar® armor blunts and slows the front portion bullet.

AUTODYN COMPUTER PREDICTIONS OF KEVLAR® ARMOR PENETRATION

A simulation very similar to that presented in Figure 2 was made with a 20 mm thick Kevlar® panel in front of the steel to test the stopping effect of the Kevlar® armor on a hunting bullet. As pointed out in the introduction, the steel is used a witness plate behind the Kevlar®. Comparison of impact craters in the steel with and without the Kevlar® gives an indication of the effect the Kevlar® has on the bullet. The AUTODYN model of the A-frame bullet, Kevlar® armor and steel witness plate is illustrated in Figure 4. Material properties are listed in Table 1. Predicted penetration of the Kevlar® is shown at three different simulation times in Figure 5. It is evident that the Kevlar® blunts the bullet and consumes a significant portion of it's' length leaving less lead and copper for steel penetration. It is interesting to note that the Kevlar® does not slow the unconsumed or back portion of the bullet which continues at the initial velocity. Figure 6 illustrates the flight of the deformed bullet after exiting the Kevlar® and its' impact on the steel witness plate. Having performed

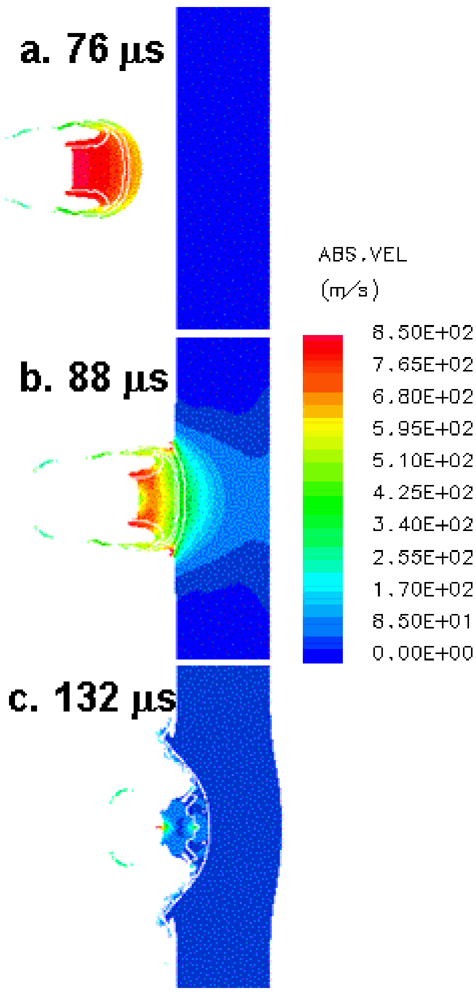

Figure 6. Continuation of the AUTODYN simulation from Figure 5 illustrating removal of the Kevlar® from the simulation and impact of the deformed bullet on the steel witness plate. Color represents absolute velocity in m/s as indicated by the color bar.

it's function, the Kevlar® is removed from the simulation at 70 μs. Figure 7 shows the predicted impact crater in the steel along with it's' dimensions. Due to the deformed configuration of the bullet on impact (Figure 6a), it makes a crater in the steel that is wider and more shallow than that produced by an undeformed bullet.

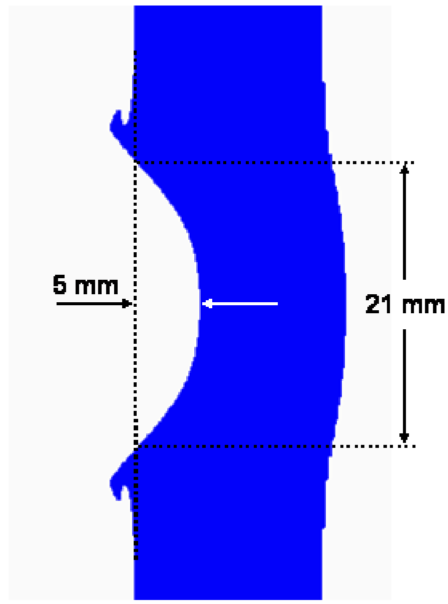

Figure 7. Impact crater dimensions from Figure 6c. Measurements are made to steel surfaces.

BALLISTIC TESTING OF BULLET IMPACT ON STEEL AND KEVLAR®/STEEL ARMOR

A series of experiments were performed in support of this project at the Sandia Ballistics Laboratory. The first tests were done with a 338 Winchester Magnum A-frame hunting bullet fired at bare steel from a Ruger M70 bolt action rifle (Figure 8).

Figure 8. 338 Winchester Magnum Ruger M70 hunting rifle.

Bullet velocity was chronographed during each shot and used in subsequent AUTODYN simulations as previously presented. The Bullet-induced crater along with a cross-section cut is illustrated in Figure 9. A water-jet process was used for the cross-section cut. The corresponding bulge on the back of the steel plate is illustrated in Figure 10.

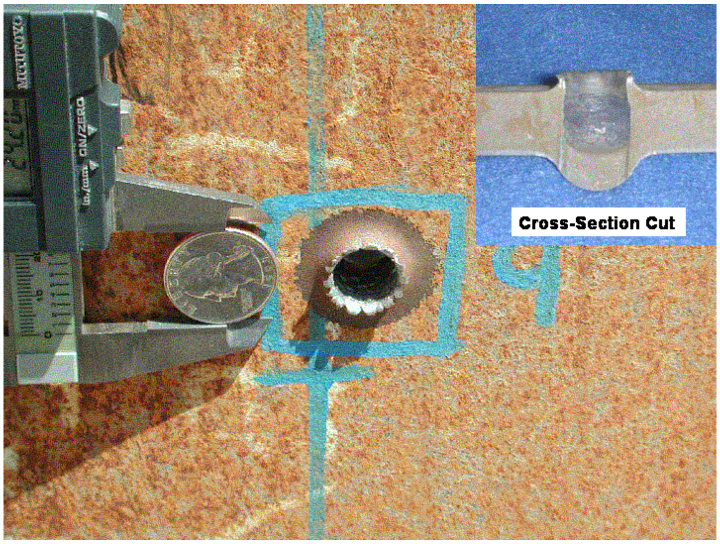

Figure 9. Bullet impact crater on steel witness plate along with a cross-section cut.

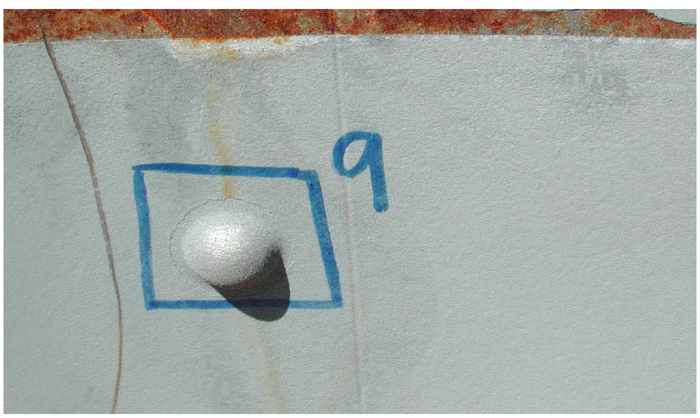

Figure 10. Bullet-induced bulge on back side of steel corresponding to impact crater.

Comparison between predicted and measured impact craters is illustrated in Figure 11. The comparison is quite good with the measured crater being ~10% wider and ~1.6% deeper than the predicted crater. Measured and predicted crater dimensions are considered close enough that this method of simulation is validated and could be used for other armor design exercises.

The next test series again employed the 338 bullet and included placement of a 20mm Kevlar® panel between the gun and the steel witness plate. The impact crater resulting when one Kevlar® panel is

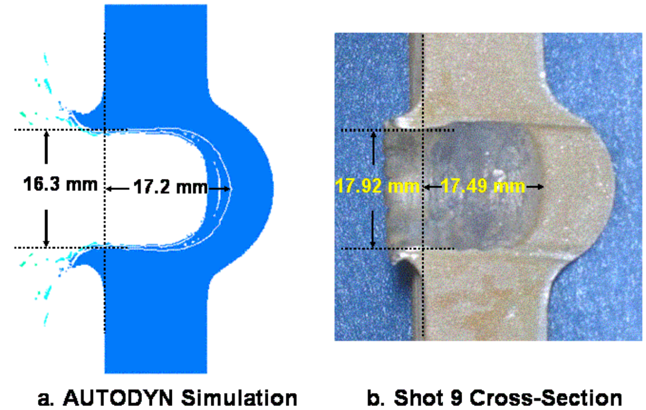

Figure 11. Comparison of AUTODYN predicted crater with experimental crater.

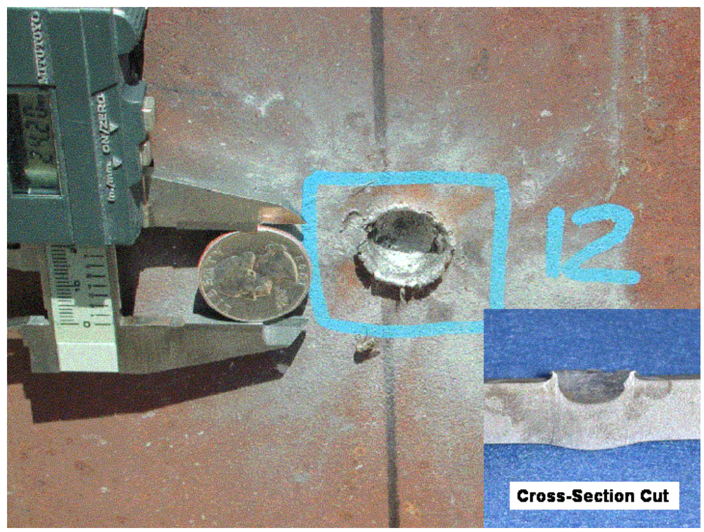

Figure 12: Bullet impact on steel plate when protected by one sheet of 20mm Kevlar®.

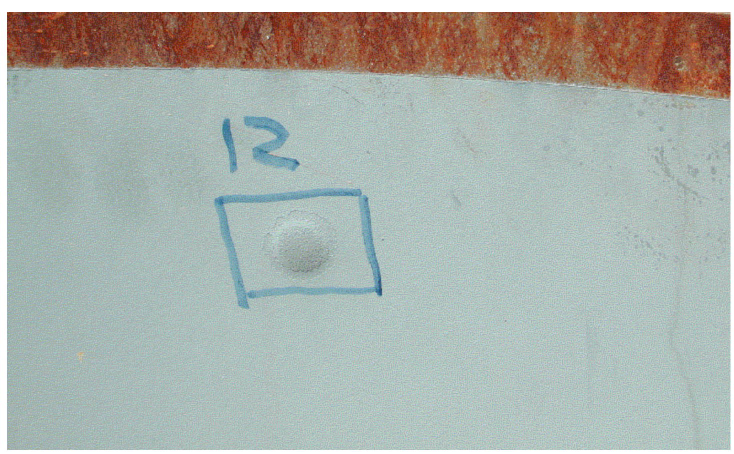

Figure 13: Back view of crater illustrated in Figure 12.

employed is illustrated in Figure 12 which also includes a crater cross-section. A photograph of the back side of the steel is shown in Figure 13.

A comparison between predicted and measured craters associated with the bullet passing through one Kevlar® panel is given in Figure 14.

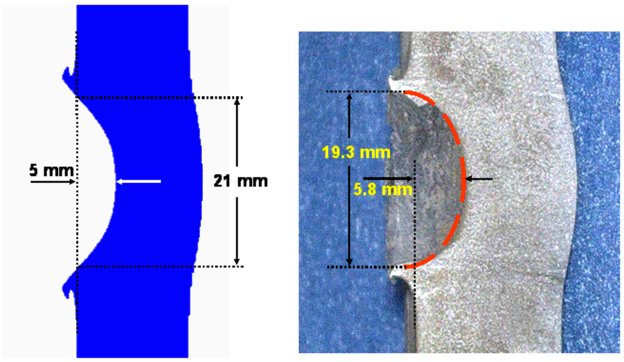

a. AUTODYN Simulation   b. Shot 12 Cross-Section

Figure 14. Comparison of predicted and measured bullet-induced craters in steel following penetration of one 20mm Kevlar® panel.

Even though the comparison is reasonable it is believed that Eulerian modeling of Kevlar® with a Von Mises strength model is quite limited and is not accurately capturing the Kevlar® behavior. This is due to the fibrous nature of the Kevlar® and the interactions of the fibers with each other as well the bonding material. This is partially illustrated by photographs of the Kevlar® board on the front and back given in Figures 15 and 16.

Figure 15. Front side of Kevlar® panel showing bullet entry hole.

A very small hole, slightly larger than the diameter of the bullet, exists on the front side of the panel as seen next to the dime in Figure 15. The exit area, affected by the bullet, is very large as seen in Figure 16 and is filled with fibrous material that is softer that the original panel but maintains some structural integrity.

The affected exit area is much larger than that predicted by AUTODYN in Figure 5b and 5c. Because a Von Mises strength model was employed the behavior illustrated in Figure 5 is metallic where the plastic region is quite small and a web develops around the deformed bulb front of the bullet and then breaks when the defined tensile strength is exceeded. The Kevlar® behavior evident from Figures 15 and 16 results from transfer of load from the front of the bullet outward into the fibrous matrix. This spreads the load, imparted by the bullet, over a large area mobilizing the strength in a large volume of material. The material model used for the Kevlar® is probably the best we can do under the circumstances but is not adequate. It seems that the nature of the Kevlar® would be more amenable to a Lagrangian material model than Eulerian. A Lagrangian composite material models for Kevlar® is available in AUTODYN (Century Dynamics, 2001). It has not yet been employed here because the large deformation of the bullet requires an Eulerian treatment. Lagrangian treatment of the bullet would likely result in mesh tangling. A logical solution would be to treat the bullet Eulerian and the Kevlar® Lagrangian with an interface polygon between the two. This was not deemed to be an adequate solution because the nodes on the interface polygon cannot be eroded as would be necessary for treatment of the large deformation and hole induced in the Kevlar® by the bullet. Future versions of AUTODYN will couple Eulerian and Lagrangian systems with Flux Corrected Transport (FCT) allowing Eulerian/Lagrangian coupling with an erodable interface.

Figure 16. Back side of Kevlar® panel where bullet exited.

CONCLUSIONS

This study has shown that the predictive capability for penetration of lead/copper bullets is quite good. It has also shown that, even though the final results are close in terms of impact crater dimensions, the predictive capability for Eulerian modeling of Kevlar® is probably not adequate and requires more development. This study has also shown that a 338 Winchester Magnum bullet is almost stopped by one Kevlar® panel 20mm thick and is stopped by 14.275 mm of steel.

REFERENCES

1. Century Dynamics, **AUTODYN User and Theory Manual**, 2001.

2. Nosler, Inc, **Nosler Reloading Guide**, 2002.